

Effect of Plasticizer and Lithium Salt Concentration in PMMA-based Composite Polymer Electrolytes

Chung-Wen Kuo¹, Wen-Bin Li¹, Pin-Rong Chen², Jian-Wei Liao², Ching-Guey Tseng¹, Tzi-Yi Wu^{2,*}

¹ Department of Chemical and Materials Engineering, National Kaohsiung University of Applied Sciences, Kaohsiung 80778, Taiwan

² Department of Chemical and Materials Engineering, National Yunlin University of Science and Technology, Yunlin 64002, Taiwan, ROC

*E-mail: wuty@yuntech.edu.tw

Received: 8 February 2013 / Accepted: 11 March 2013 / Published: 1 April 2013

Blended polymer electrolytes with poly(methyl methacrylate) (PMMA) were prepared with various propylene carbonate (PC) plasticizer concentrations and lithium perchlorate (LiClO₄) ratio by the solution-casting technique. Fourier transform infrared studies show the evidence of the complexation between PMMA, LiClO₄, and PC. The composite polymer electrolytes show good thermal property, which are confirmed by thermo gravimetric analysis (TGA) and differential scanning calorimetry (DSC). PC is added to the PMMA–LiClO₄ blend polymer electrolytes as plasticizer to enhance the conductivity, and the highest conductivity obtained is $5.64 \times 10^{-3} \text{ S cm}^{-1}$ at 80 °C for PC mixture system. Moreover, the maximum conductivity of polymer electrolyte (PMMA:PC:LiClO₄:SiO₂ (wt. ratio) = 299:556:128:17) is up to 8.91 mS cm⁻¹ at 90 °C by optimizing the composition of the polymers, salts, plasticizer, and filler, and the temperature dependence of the conductivity of polymer electrolytes obeys the Vogel–Tamman–Fulcher (VTF) relationship.

Keywords: Conductivity, polymer electrolytes, Fourier transform infrared spectroscopy, PMMA blends, Vogel–Tamman–Fulcher

1. INTRODUCTION

Polymer electrolytes have been found to have a great deal of advantages in replacing conventional liquid electrolytes. These advantages includes high specific energy, high energy density, leak proof, high ionic conductivity, wide electrochemical stability windows, light, solvent free condition and easy processability [1]. The interest in the study of polymer electrolyte system is due to the potential application of these materials in a great variety of electrochemical devices such as high energy density batteries, fuel cells, sensors, and electrochromic devices [2-12]. Generally, there are three types of polymer electrolytes: solid polymer electrolytes (SPEs), gel polymer electrolytes

(GPEs), and composite polymer electrolytes (CPEs) [13-20]. The GPE is fabricated in an anhydrous environment by dissolving host polymer into a highly hygroscopic liquid electrolyte and casting the polymer solution at elevated temperatures (120–140 °C), followed by cooling the cast thin solution to form the gel electrolyte film [21]. Among the polymer matrixes that are promising for the application in GPE, polyacrylonitrile (PAN) [22,23], poly(vinylidene fluoride) (PVDF) [24,25], poly(methyl methacrylate) (PMMA) [26], and poly(ethylene oxide) (PEO) [27-30] based polymers have been most extensively studied. Poly(methyl methacrylate) (PMMA)-based electrolyte has a special significance because of its well-known chemistry and cheaper method of processing them as laminates. However, its low conductivity at room temperature due to the formation of crystalline precludes it from practical applications. Consequently, much effort has been devoted to investigate amorphous polymeric materials with high ionic conductivity at room temperature with good mechanical and thermal properties. These include introducing new polymer host [31], blending [32], plasticization [33], and filler addition [34].

Polymer blending is one of the most contemporary techniques for designing new polymeric materials with superior properties, which is unattainable by single component. In general, the blending lithium salts (LiAsF_6 , LiClO_4 , LiCF_3SO_3 , LiBF_4 , and $\text{LiN}(\text{SO}_2\text{CF}_3)_2$) are added so as to increase the amorphicity and the introduction of conducting moieties into the matrix. Among these salts, LiClO_4 shows low lattice energy, which is effective for improvement of the ionic conductivity [35]. Moreover, plasticizer such as propylene carbonate (PC) is preferred for our work because of its high dielectric constant ($\epsilon_r = 64.4$ at 25 °C) and low molecular weight which will enhance the dissociation of ion pairs of the salt. Therefore, the electrolyte could be used over a wide range of temperature [36]. Furthermore, the addition of SiO_2 filler which provides high surface area not only enhances the mechanical properties but also increases ionic conductivity of the CPEs [37]. In the present work, hybrid solid polymer electrolyte films that consist of PMMA, LiClO_4 , PC, and SiO_2 filler are prepared using solvent casting technique. The effect of PMMA, LiClO_4 , PC, and SiO_2 blend ratio on the ionic conductivity and thermal properties has been investigated to optimize the appropriate concentration of salt, plasticizer, and filler at which the electrolyte provides maximum conductivity. Moreover, DSC measurement provides a quantitative study of thermal transitions of matrix polymer in polymer electrolytes by heating the polymer sample and an inert reference. Thermogravimetric analysis (TGA) is another versatile thermal analysis to investigate the thermal properties of SPEs as a function of change in temperature by determining the thermal stability of polymer electrolytes. The prepared polymer electrolytes are characterized by FTIR, ac impedance, TGA, and DSC for the complexation, conductivity, thermal stability, and phase transition properties, respectively. The temperature dependence of ionic conductivity is extensively used in the study of ionic conduction behaviors for polymer electrolytes.

2. EXPERIMENTAL

2.1. Materials

The host polymer, PMMA ($M_w=35,000$) obtained from ACROS organics was dried at 373K under vacuum for 10 h, while doping salt, LiClO_4 , was obtained from Aldrich and was dried at 343K

under vacuum for 24 h. Plasticizer propylene carbonate (PC) (Alfa Aesar) was used without further purification, and fumed silica (SiO_2) with 7 nm particle size was obtained from Aldrich.

2.2. Preparation of thin films

Prior to the preparation of the polymer electrolytes, LiClO_4 was dried at 100 °C for 1 h to eliminate trace amounts of water in the material. Table 1, Table 2, and Table 3 show the compositions and designations of particular polymer electrolytes, PC90, PC100, PC110, PC120, and PC130 represent PMMA:PC: LiClO_4 weight ratio of polymer blends are 37:47:16, 35:50:15, 33:53:14, 32:55:13, and 30:57:13, respectively, whereas Li150, Li200, Li250, Li300, Li350, and Li400 indicate PMMA:PC: LiClO_4 weight ratio of polymer blends are 36:56:8, 35:55:10, 34:54:12, 33:53:14, 33:51:16, and 32:50:18, respectively, Si21, S19, and S17 imply the PMMA:PC: LiClO_4 : SiO_2 weight ratio of polymer blends are 361:464:154:21, 327:514:140:19, and 299:556:128:17, respectively.

Table 1. Polymer electrolytes with various PC concentrations.

	PMMA (g)	PC (g)	LiClO_4 (g)	PMMA:PC: LiClO_4 (wt.%)
PC90	0.70	0.90	0.30	37:47:16
PC100	0.70	1.00	0.30	35:50:15
PC110	0.70	1.10	0.30	33:53:14
PC120	0.70	1.20	0.30	32:55:13
PC130	0.70	1.30	0.30	30:57:13

Table 2. Polymer electrolytes with various LiClO_4 concentrations.

	PMMA (g)	PC (g)	LiClO_4 (g)	PMMA:PC: LiClO_4 (wt.%)
Li150	0.70	1.10	0.150	36:56:8
Li200	0.70	1.10	0.200	35:55:10
Li250	0.70	1.10	0.250	34:54:12
Li300	0.70	1.10	0.300	33:53:14
Li350	0.70	1.10	0.350	33:51:16
Li400	0.70	1.10	0.400	32:50:18

Table 3. SiO_2 -containing polymer electrolytes.

	PMMA (g)	PC (g)	LiClO_4 (g)	SiO_2 (g)	PMMA:PC: LiClO_4 : SiO_2 (wt. ratio)
Si21	0.70	0.90	0.30	0.04	361:464:154:21
Si19	0.70	1.10	0.30	0.04	327:514:140:19
Si17	0.70	1.30	0.30	0.04	299:556:128:17

Appropriate weight percentage of PMMA, PC, LiClO_4 , and SiO_2 filler were dissolved in DMF. The solution was stirred for 24 h at room temperature to obtain a homogenous mixture. The solution

was then poured into a Petri dish and allowed to evaporate slowly inside a hood. This procedure yields stable and free standing thin films. The films were dried in a vacuum oven at 333 K under a pressure of 10^{-3} Torr for 24 h. The resulting films were visually examined for their dryness and free-standing nature.

2.3. Measurements

FTIR studies were carried by using Perkin-Elmer FTIR Spectrophotometer Spectrum RX1. It was recorded in the range of 4,000 and 400 cm^{-1} , with resolution 4 cm^{-1} . Thermal properties of the membranes were investigated by differential scanning calorimetry, DSC, and thermal gravimetric analysis, TGA. The experiments were performed at a scanning rate of 20°C/min in a flux of nitrogen for TGA and 10°C/min in a flux of nitrogen for DSC. The thermal stabilities were measured with TGA (Perkin-Elmer, 7 series thermal analysis system), while the thermal transition temperature of each polymer electrolyte was analyzed using a differential scanning calorimeter (DSC, Perkin-Elmer Pyris 1). The ionic conductivity (σ) of the gel polymer electrolytes was determined by AC impedance spectroscopy (CHI 627D). The membrane was sandwiched between two parallel stainless steel discs ($d = 1$ cm). The thicknesses of the films were measured using micrometer screw gauge. Temperatures were controlled with an accuracy of 0.5 °C and were kept constant during each measurement. The frequency ranged from 100 kHz to 10 Hz at a perturbation voltage of 10 mV. The ionic conductivity was calculated from the electrolyte resistance (R_b) obtained from the intercept of the Nyquist plot with the real axis, the membrane thickness (l), and the electrode area (A) according to the equation:

$$\Lambda = \frac{l}{A} \cdot R_b \quad (1)$$

3. RESULTS AND DISCUSSION

3.1. FTIR studies

Infrared spectral (IR) analysis is a powerful tool for identifying the nature of bonding and different functional groups present in a sample by monitoring the vibrational energy levels of the molecules, which are essentially the fingerprint of different molecules [38]. Fig. 1 shows the FTIR spectra of neat PMMA, neat PC, PC90, PC100, PC110, PC120, and PC130, a band can be observed at 1,736 cm^{-1} , which is due to the C=O asymmetric stretching of the carbonyl group in pure PMMA, the bands at 2952, 1433, and 1195 cm^{-1} correspond to -CH₃ stretching, -OCH₃ asymmetric bending, and -CH₂ twisting of PMMA, respectively. With the addition of lithium salts to PMMA, the C=O stretching band broadened and shifted to lower wave numbers (1726 cm^{-1} , Fig 2). This indicates that there is an interaction between the carbonyl group of PMMA ester and LiClO₄ via a coordinate bond, and hence complexation has occurred. The -OCH₃ asymmetric stretch bands of PMMA at 1,433 cm^{-1} are found to exist at the same wavenumbers in the polymer complexes and the pure PMMA, indicating the coordination to the salt did not occur at -OCH₃ group.

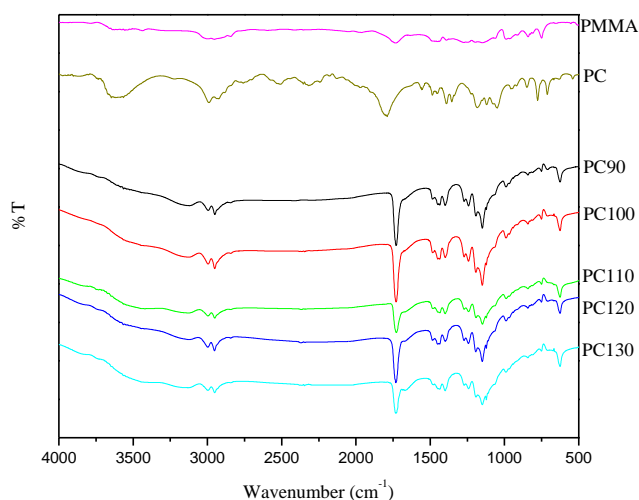


Figure 1. FT-IR spectra of neat PMMA, neat PC, and gel polymer electrolytes with various concentrations of PC.

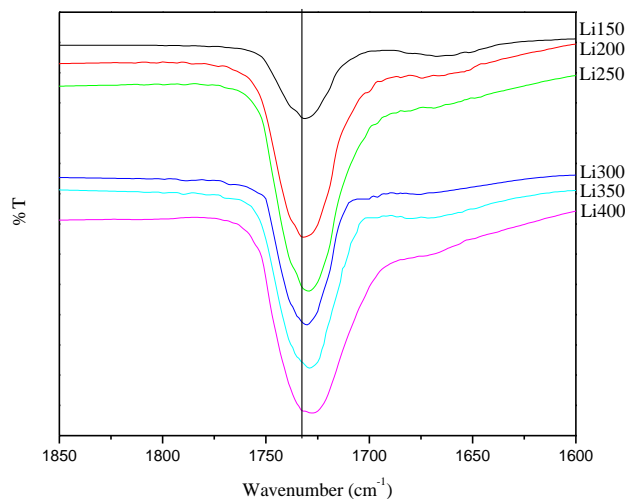


Figure 2. The FTIR spectra of PMMA C=O stretching in the polymer electrolytes with various concentrations of LiClO₄.

3.2. Conductivity studies

The ionic conductivity depends on overall mobility of ion and polymer, which is determined by the free volume around the polymer chain. Generally, the ionic conductivity of polymer solid electrolytes increases with temperature due to the higher segmental motion of polymer chain in the amorphous phase. The investigation of conductivity contain three topics in this study, (1) the conductivity of PMMA-LiClO₄-PC polymer electrolytes by blending various PC concentrations, (2) the conductivity of PMMA-LiClO₄-PC polymer electrolytes by blending various LiClO₄ concentrations, (3) the conductivity of PMMA-LiClO₄-PC-SiO₂ polymer electrolytes.

The temperature dependence of the ionic conductivity of the polymer electrolytes is generally following by an Arrhenius Eq. (2) [39,40]

$$\sigma = \sigma_{\infty} \left[\frac{-E_a}{k_B T} \right] \quad (2)$$

where E_a is the activation energy for electrical conduction (which indicates the energy needed for an ion to jump to a free hole), σ_{∞} is the maximum electrical conductivity (that it would have at infinite temperature), and k_B is the Boltzman constant. However, some observed temperature dependence of conductivity are not linear but polynomial ($n = 2$ or $n = 3$), and are often best fitted by the empirical Vogel–Tammann–Fulcher (VTF) equation [41-50],

$$\sigma = \frac{\sigma_0}{\sqrt{T}} \exp\left[\frac{-B'}{k_B(T-T_0)}\right] \quad (3)$$

or Fulcher equation [41-50].

$$\sigma = \sigma_0 \exp\left[\frac{-B'}{(T-T_0)}\right] \quad (4)$$

where σ_0 is a constant that is proportional to the number of carrier ions; B' is the pseudo-activation energy for the redistribution of the free volume; k_B is the Boltzmann constant (1.38×10^{-23} J K^{-1}); E_a is the activation energy, and T_0 is a reference temperature, normally associated with the ideal T_g at which the free volume is zero or with the temperature at which the configuration entropy becomes zero [51].

Eq. 5 is Eyring equation, a linear relationship is obtained from the plot of $\ln\left(\frac{\sigma h}{k_B T}\right)$ vs. $1000/T$, the slope is $-\Delta H$, and the intercept is ΔS . Accordingly, the Arrhenius active energy (E_a), entropy (ΔS), and enthalpy (ΔH) can be estimated from Arrhenius equation and Eyring equation [52-57]:

$$R \ln\left(\frac{\sigma h}{k_B T}\right) = \frac{-\Delta H}{T} + \Delta S \quad (5)$$

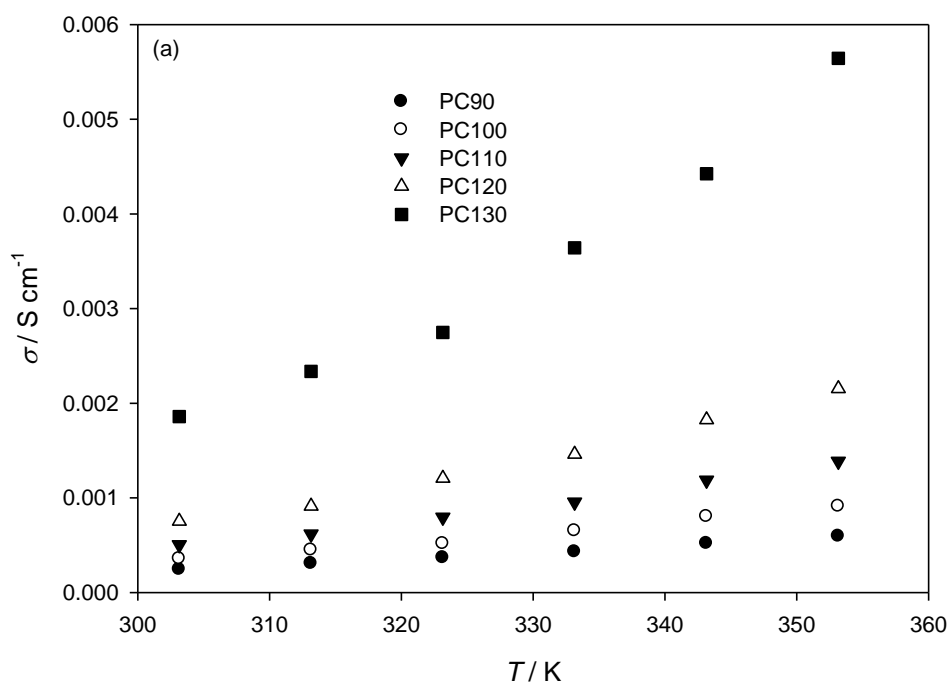
where h is Planck's constant (6.626×10^{-34} J s), ΔH is the enthalpy of electrolyte, ΔS is the entropy of electrolyte.

3.2.1. Conductivity of PMMA-LiClO₄-PC polymer electrolytes by blending various PC concentrations

Fig. 3(a) shows the effects of PC on the conductivity of the conducting PMMA–LiClO₄ sample. It is observed that the ionic conductivity of the salt polymer blend electrolyte increases further upon the addition of PC plasticizer.

Table 4. Fitted parameters of composite polymer electrolytes for $\ln \sigma = A + B (10^3 \times 1/T)$, σ , conductivity (S cm⁻¹).

Polymer electrolytes		A	B	R ²
PC	PC90	-2.0534	-1.8957	0.9988
	PC100	-1.2087	-2.0421	0.9953
	PC110	-0.3147	-2.2093	0.9985
	PC120	0.3955	-2.3051	0.9974
	PC130	1.4892	-2.3667	0.9927
Li	Li150	-1.4459	-2.4627	0.9923
	Li200	2.0288	-3.4829	0.9989
	Li250	-0.7718	-2.4133	0.9938
	Li300	-0.2916	-2.2159	0.9985
	Li350	4.7096	-4.0336	0.9977
	Li400	8.0646	-5.2675	0.9963
SiO ₂	Si21	5.6128	-4.1055	0.9873
	Si19	8.2437	-4.7598	0.9957
	Si17	2.2845	-2.5665	0.9864



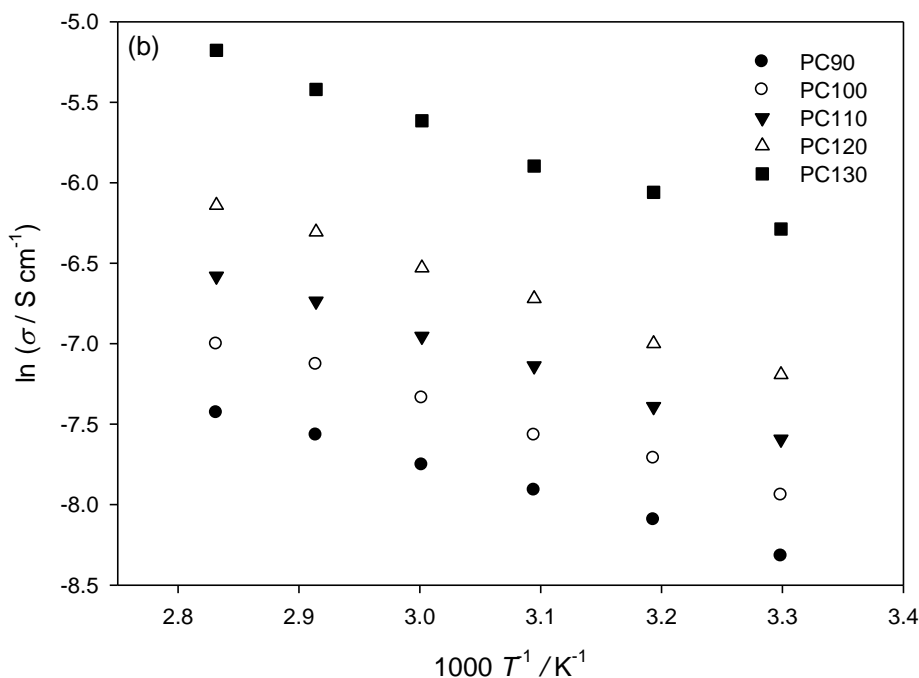


Figure 3. Ionic conductivities of gel polymer electrolytes PC90, PC100, PC110, PC120, and PC130. (a) σ vs. T plot; (b) $\ln \sigma$ vs. $1000 T^{-1}$ plot.

For 57 wt.% PC, the plasticized polymer blend system achieves maximum conductivity, with a value of $5.64 \times 10^{-3} \text{ S cm}^{-1}$ at 80 °C. Fig. 3(b) shows the $\ln \sigma$ versus $1/T$ plots of these polymer electrolytes, some observed temperature dependence of $\ln \sigma$ versus $1/T$ are not linear but polynomial ($n = 2$ or $n = 3$), and the conductivity of polymer electrolyte are often best fitted by the empirical Vogel–Tammann–Fulcher (VTF) or Fulcher equation, the VTF fitting parameters of the ionic conductivity for these polymer electrolytes are summarized in Table 5. The Arrhenius active energy (E_a), entropy (ΔS), and enthalpy (ΔH) can be estimated from Arrhenius equation and Eyring equation, and are summarized in Table 6. E_a , ΔS , and ΔH increases with increasing concentration of PC, depicting the addition of PC decreases E_a and facilitates the lithium ion hopping in polymer backbone.

3.2.2. Conductivity of PMMA-LiClO₄-PC polymer electrolytes by blending various LiClO₄ concentrations

Fig. 4(a) shows the σ vs. T plot of polymer electrolytes prepared by blending 0.15, 0.2, 0.25, 0.3, 0.35, and 0.4 g LiClO₄ with 0.7 g PMMA and 1.1 g PC. Fig. 4(b) shows the $\ln \sigma$ versus $1/T$ plots of these polymer electrolytes, some observed temperature dependence of $\ln \sigma$ versus $1/T$ are not linear but polynomial ($n = 2$ or $n = 3$), and the conductivity of polymer electrolyte are often best fitted by the empirical Vogel–Tammann–Fulcher (VTF) or Fulcher equation, the VTF fitting parameters of the ionic conductivity for these polymer electrolytes are summarized in Table 5. Fig. 4(c) shows the

temperature dependence of conductivity at various LiClO_4 concentrations, it can be seen that the conductivity of these polymer electrolyte increases with increasing weight percentage of LiClO_4 , goes through a maximum ($1.39 \times 10^{-3} \text{ S cm}^{-1}$ at 80°C), and then goes down to the specific conductivity ($1.01 \times 10^{-3} \text{ S cm}^{-1}$ at 80°C). This could be due to increase of charge carrier up to the optimum concentration (14 wt.% of LiClO_4) which gives the highest ionic conductivity among the various polymer electrolytes characterized. As the concentration is increased above the optimum concentration, the conductivity is found to decrease that could be ascertained due to formation of ion pairs or ion clusters which restricts the mobility of the charge carriers in the matrix [58]. The Arrhenius active energy (E_a), entropy (ΔS), and enthalpy (ΔH) can be estimated from Arrhenius equation and Eyring equation, and are summarized in Table 6. Li300 shows lowest E_a , implying the addition of 14 wt.% LiClO_4 facilitates the lithium ion hopping in polymer matrix.

Table 5. VTF equation parameters of conductivity for composite polymer electrolytes. ($\sigma = \sigma_0 \exp[-B^2/(T - T_0)]$).

	Polymer electrolytes	σ_0 (S cm ⁻¹)	T_0 (K)	B^2 (K) ^a	R^2
PC	PC90	0.007	164.6	457.5	0.999
	PC100	0.011	163.6	486.0	0.999
	PC110	0.017	174.3	457.8	0.999
	PC120	0.033	169.2	508.3	0.999
	PC130	0.094	160.7	561.6	0.999
Li	Li150	0.005	155.5	636.7	0.999
	Li200	0.041	153.6	937.3	0.999
	Li250	0.010	156.5	599.0	0.999
	Li300	0.024	160.0	556.3	0.999
	Li350	0.164	163.8	946.3	0.999
	Li400	0.140	201.5	754.4	0.999
SiO ₂	Si21	0.100	211.5	526.3	0.999
	Si19	0.710	167.8	954.6	0.999
	Si17	0.166	149.1	668.4	0.999

^a Activation energy (kJ mol⁻¹).

3.2.3. Conductivity of PMMA-LiClO₄-PC-SiO₂ polymer electrolytes

Fig. 5(a) shows the variation of conductivity with various weight percentage of SiO₂ (Si21: 2.1 wt % SiO₂, Si19: 1.9 wt % SiO₂, Si17: 1.7 wt % SiO₂) at room temperature. Si17 shows a maximum conductivity of $8.91 \times 10^{-3} \text{ S cm}^{-1}$, corresponding to the sample with a 1.7 wt.% SiO₂ in PMMA-LiClO₄-PC-SiO₂ polymer complex. The conductivity does not rise with increasing concentration of SiO₂, this behavior is a direct consequence of a high concentration of the fumed silica which will lead to aggregate of SiO₂ and formed a crystal like particle on the surface [59]. Fig. 5(b) shows the $\ln \sigma$ versus $1/T$ plots of these polymer electrolytes, some observed temperature dependence of $\ln \sigma$ versus $1/T$ are not linear but polynomial ($n = 2$ or $n = 3$), and the conductivity of polymer electrolyte are often

best fitted by the empirical Vogel–Tammann–Fulcher (VTF) or Fulcher equation, the VTF fitting parameters of the ionic conductivity for these polymer electrolytes are summarized in Table 5.

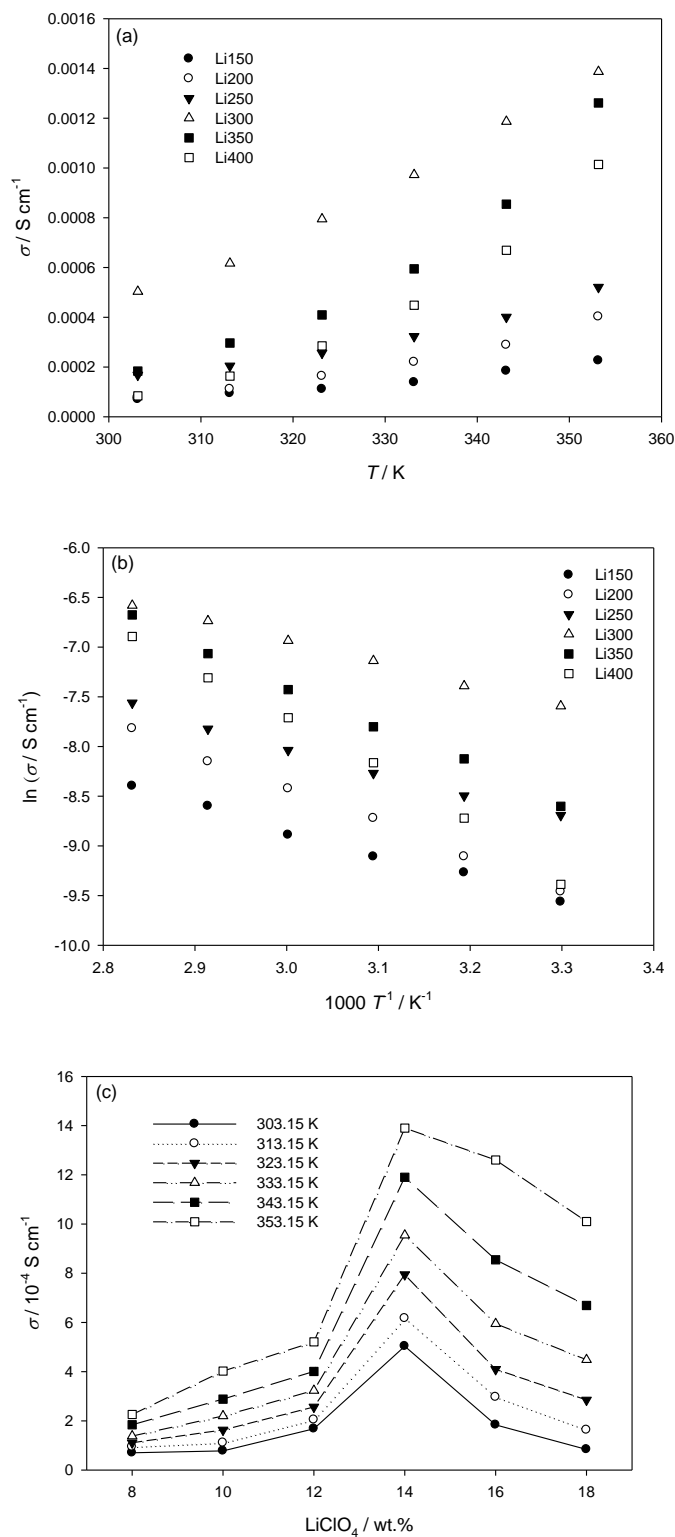


Figure 4. Ionic conductivities of gel polymer electrolytes Li150, Li200, Li250, Li300, Li350, and Li400. (a) σ vs. T plot; (b) $\ln \sigma$ vs. $1000 T^{-1}$ plot; (c) plot of conductivity vs. various LiClO_4 concentration.

The Arrhenius active energy (E_a), entropy (ΔS), and enthalpy (ΔH) can be estimated from Arrhenius equation and Eyring equation, and are summarized in Table 6, there is no significant relationship of E_a , ΔS , and ΔH by blending polymer electrolytes with various SiO_2 weight percentage.

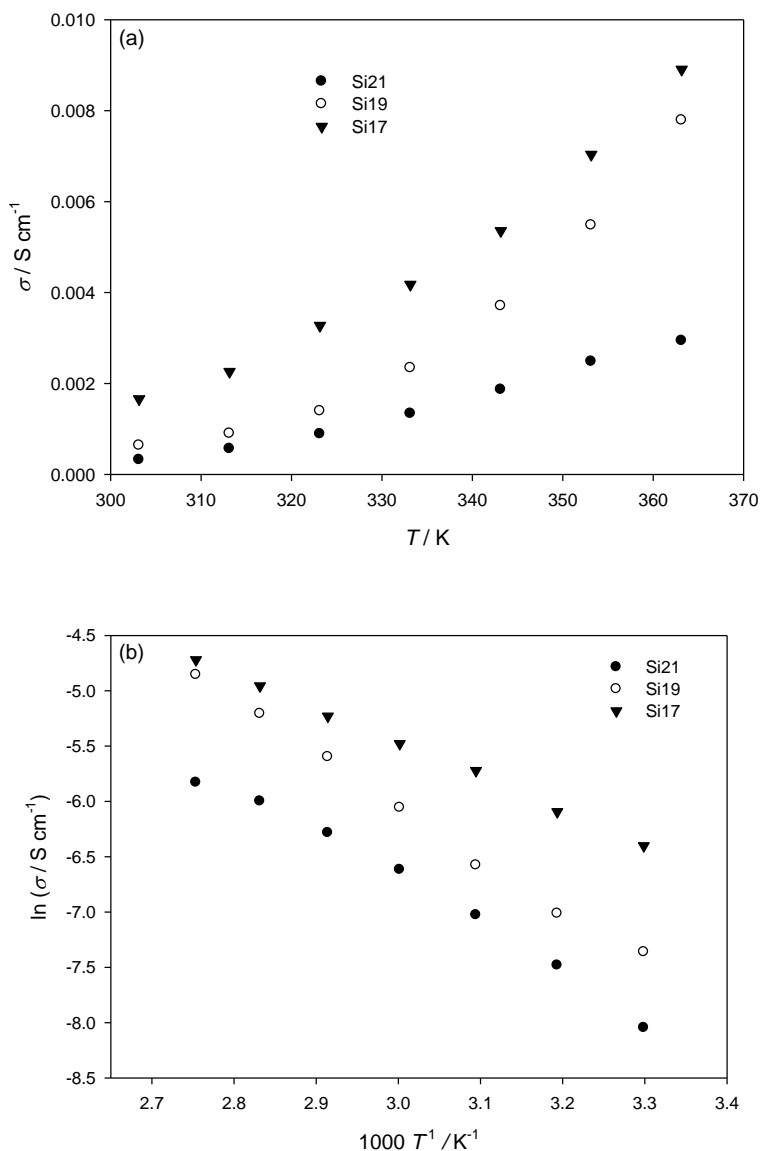


Figure 5. Ionic conductivities of gel polymer electrolytes Si21, Si19, and Si17. (a) σ vs. T plot; (b) $\ln \sigma$ vs. $1000 T^{-1}$ plot.

3.3. Thermal properties

Thermal stability was represented by determining the weight loss of the sample after heating over the temperature range of 30 ~ 800 °C using Thermal gravimetric analyzer (TGA). The TGA curves of PMMA–LiClO₄-PC samples with different LiClO₄ concentrations are depicted in Fig. 6. The polymer electrolytes Li150, Li200, Li250, Li300, Li350, and Li400 are found to be stable up to 255, 252,

247, 249, 228, and 223 °C, respectively, with weight loss of about 10 %, implying these polymer electrolytes show good thermal stability. The DSC thermograms of PMMA–LiClO₄-PC blend polymer electrolytes are shown in Fig. 7, an endothermic transition T_g is observed.

Table 6. The E_a , ΔS and ΔH evaluated by Eyring equation and the relationships of σ vs. T .

	Polymer electrolytes	$E_a/$ kJ mole ⁻¹	$\Delta S/$ J mole ⁻¹ K ⁻¹	$\Delta H/$ kJ mole ⁻¹
PC	PC90	15.76	-271.07	13.04
	PC100	16.98	-264.04	14.26
	PC110	18.37	-256.61	15.65
	PC120	19.16	-250.71	16.45
	PC130	19.68	-241.61	16.96
Li	Li150	20.47	-266.02	17.76
	Li200	28.96	-237.13	26.24
	Li250	20.06	-260.41	17.35
	Li300	18.42	-256.42	15.71
	Li350	33.54	-214.84	30.82
	Li400	43.79	-186.95	41.08
SiO ₂	Si21	34.13	-207.45	31.38
	Si19	39.57	-185.57	36.82
	Si17	21.34	-235.12	18.58

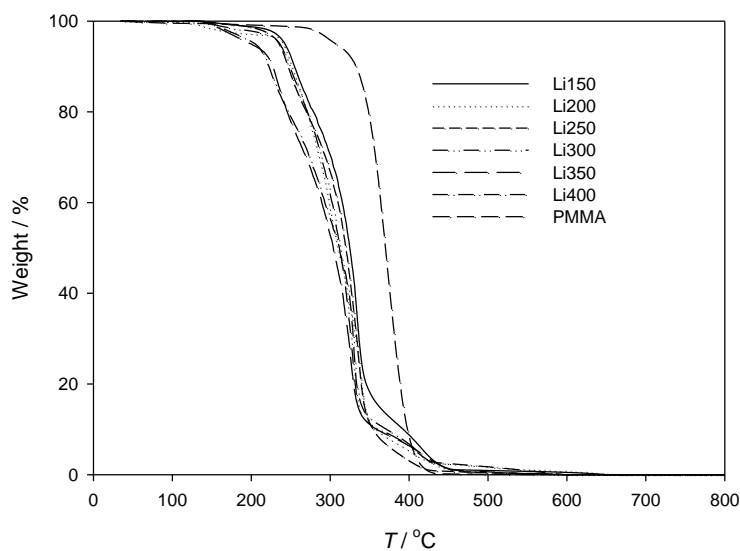


Figure 6. The TGA curves of polymer electrolytes with various LiClO₄ concentrations.

Apparently, only one T_g is displayed for PMMA–LiClO₄-PC polymer blend and this indicates the homogeneous behavior of the polymer electrolyte [60]. It is clear that PMMA–LiClO₄-PC electrolytes have T_g between 68 and 75 °C at various LiClO₄ concentrations. In addition, T_g increases upon incorporation of lithium salt gradually due to the interaction between PMMA and LiClO₄. T_g is defined as the transition of temperature from glassy state to rubbery state. Beyond this transition, a

long range molecular motion occurs and thus the degree of rotational freedom increases. As a result, the increase in T_g indicates in the hardening of the polymer backbone upon incorporation of lithium salt into PMMA gradually.

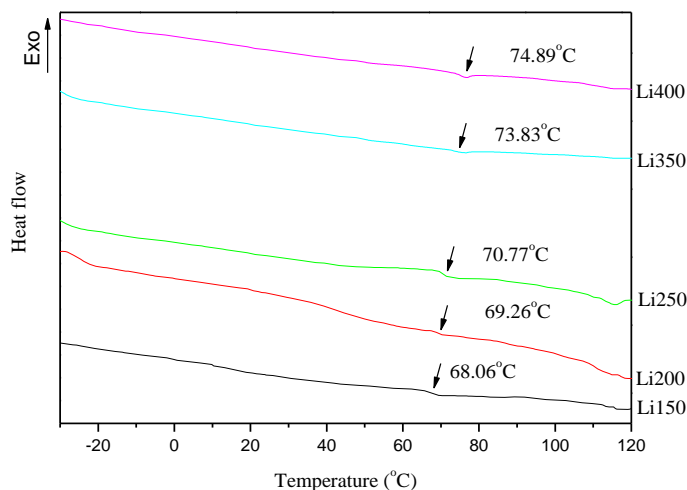


Figure 7. The DSC thermograms of polymer electrolytes with various LiClO₄ concentrations.

4. CONCLUSIONS

Polymer electrolyte systems consisting of PMMA-LiClO₄-PC for various plasticizer and salt concentrations have been prepared using solvent casting technique. Complexation taking place in PMMA-LiClO₄-PC polymer electrolytes with various LiClO₄ salt concentrations have been confirmed from FTIR studies. Ionic conductivity studies reveal that a PMMA-LiClO₄-PC polymer complex (PMMA:PC:LiClO₄ (wt. %) = 30:57:13) has the highest ionic conductivity of $5.64 \times 10^{-3} \text{ S cm}^{-1}$ at 80 °C, whereas a PMMA-LiClO₄-PC-SiO₂ polymer complex (PMMA:PC:LiClO₄:SiO₂ (wt. ratio) = 299:556:128:17) has the highest ionic conductivity of $7.04 \times 10^{-3} \text{ S cm}^{-1}$ at 80 °C. The temperature dependence conductivity of the PMMA-LiClO₄-PC-SiO₂ blended polymer electrolytes obeys the VTF relationship, and the active energy (E_a), entropy (ΔS), and enthalpy (ΔH) of polymer electrolytes are estimated. The thermal behaviours of the polymer electrolytes are ascertained from TGA and DSC, TGA results showed that the amount of LiClO₄ has a significant effect on the thermal stability of polymer complexes, whereas DSC results showed that the amount of LiClO₄ in polymer electrolytes has distinct variations on the phase transition temperature.

ACKNOWLEDGEMENTS

The financial support of this work by the National Science Council of Taiwan under NSC 101-2221-E-151-058, NSC 99-2218-E-151-003, and NSC101-2218-E-224-002 is gratefully acknowledged.

References

1. J.Y. Kim, S.H. Kim, *Solid State Ionics*, 124 (1999) 91.
2. J. Gao, J. Liu, W. Liu, B. Li, Y. Xin, Y. Yin, Z. Zou, *Int. J. Electrochem. Sci.*, 6 (2011) 6115.

3. L.C. Xuan, Y.X. An, W. Fang, L.X. Liao, Y.L. Ma, Z.Y. Ren, G.P. Yin, *Int. J. Electrochem. Sci.*, 6 (2011) 6590.
4. M.S.M. Eldin, M.A. Abu-Saied, A.A. Elzatahry, K.M. El-Khatib, E.A. Hassan, K.M. El-Sabbah, *Int. J. Electrochem. Sci.*, 6 (2011) 5417.
5. J.H. Kim, S.K. Kim, Y.Z. You, D.I. Kim, S.T. Hong, H.C. Suh, K.S. Weil, *Int. J. Electrochem. Sci.*, 6 (2011) 4365.
6. A. Anis, S.M. Al-Zahrani, A.K. Banthia, S. Bandyopadhyay, *Int. J. Electrochem. Sci.*, 6 (2011) 2461.
7. A. Anis, S.M. Al-Zahrani, A.K. Banthia, S. Bandyopadhyay, *Int. J. Electrochem. Sci.*, 6 (2011) 2652.
8. W.H. Chen, T.H. Ko, J.H. Lin, C.H. Liu, C.W. Shen, C.H. Wang, *Int. J. Electrochem. Sci.*, 6 (2011) 2192.
9. C.H. Wan, J.M. Wei, M.T. Lin, C.H. Lin, *Int. J. Electrochem. Sci.*, 6 (2011) 889.
10. B.C. Ng, H.Y. Wong, K.W. Chew, Z. Osman, *Int. J. Electrochem. Sci.*, 6 (2011) 4355.
11. P.C. Barbosa, M. Fernandes, S.M.F. Vilela, A. Goncalves, M.C. Oliveira, E. Fortunato, M.M. Silva, M.J. Smith, R. Rego, V.D. Bermudez, *Int. J. Electrochem. Sci.*, 6 (2011) 3355.
12. T.Y. Wu, H.C. Wang, S.G. Su, S.T. Gung, M.W. Lin, C.B. Lin, *J. Chin. Chem. Soc.*, 57 (2010) 44.
13. A.M. Stephan, K.S. Nahm, *Polymer*, 47 (2006) 5952.
14. J.C. Cruz, V. Baglio, S. Siracusano, V. Antonucci, A.S. Arico, R. Ornelas, L. Ortiz-Frade, G. Osorio-Monreal, S.M. Duron-Torres, L.G. Arriaga, *Int. J. Electrochem. Sci.*, 6 (2011) 6607.
15. T.Y. Wu, B.K. Chen, L. Hao, Y.C. Lin, H.P. Wang, C.W. Kuo, I.W. Sun, *Int. J. Mol. Sci.*, 12 (2011) 8750.
16. M.R. Johan, L.M. Ting, *Int. J. Electrochem. Sci.*, 6 (2011) 4737.
17. R.C. Agrawal, Y.K. Mahipal, *Int. J. Electrochem. Sci.*, 6 (2011) 867.
18. N.A. Aini, M.Z.A. Yahya, A. Lepit, N.K. Jaafar, M.K. Harun, A.M.M. Ali, *Int. J. Electrochem. Sci.*, 7 (2012) 8226.
19. H.N. Su, B.J. Bladergroen, S. Pasupathi, V. Linkov, S. Ji, *Int. J. Electrochem. Sci.*, 7 (2012) 4223.
20. S. Siracusano, V. Baglio, M.A. Navarra, S. Panero, V. Antonucci, A.S. Arico, *Int. J. Electrochem. Sci.*, 7 (2012) 1532.
21. S.S. Zhang, K. Xu, T.R. Jow, *Solid State Ion.*, 158 (2003) 375.
22. S. Rajendran, R.S. Babu, P. Sivakumar, *Ionics*, 14 (2008) 149.
23. X.H. Flora, M. Ulaganathan, S. Rajendran, *Int. J. Electrochem. Sci.*, 7 (2012) 7451.
24. M.S. Mohy Eldin, M.A. Abu-Saied, A.A. Elzatahry, K.M. El-Khatib, E.A. Hassan, M.M. El-Sabbah, *Int. J. Electrochem. Sci.*, 6 (2011) 5417.
25. N. Ataollahi, A. Ahmad, H. Hamzah, M.Y.A. Rahman, N.S. Mohamed, *Int. J. Electrochem. Sci.*, 7 (2012) 6693.
26. K.W. Chew, K.W. Tan, *Int. J. Electrochem. Sci.*, 6 (2011) 5792.
27. S. Ibrahim, M.R. Johan, *Int. J. Electrochem. Sci.*, 6 (2011) 5565.
28. E.M. Fahmi, A. Ahmad, N.N.M. Nazeri, H. Hamzah, H. Razali, M.Y.A. Rahman, *Int. J. Electrochem. Sci.*, 7 (2012) 5798.
29. S. Ibrahim, M.R. Johan, *Int. J. Electrochem. Sci.*, 7 (2012) 2596.
30. M.R. Johan, S.M.M. Yasin, S. Ibrahim, *Int. J. Electrochem. Sci.*, 7 (2012) 222.
31. K. Sawai, Y. Iwakoshi, T. Ohzuhu, *Solid State Ionics*, 69 (1994) 273.
32. S. Rajendra, M.R. Prabhu, M. Rani, *Int. J. Electrochem. Sci.*, 3 (2008) 282.
33. D.K. Pradhan, R.P. Choudhary, B.K. Samantaray, N.K. Karan, R.S. Katiyar, *Int. J. Electrochem. Sci.*, 2 (2007) 861.
34. K.S. Ji, H.S. Moon, J.W. Kim, J.W. Park, *J. Power Sources*, 117 (2003) 124.
35. Y. Tominaga, N. Takizawa, H. Ohno, *Electrochim. Acta*, 45 (2000) 1285.
36. R. Kumar, J.P. Sharma, S.S. Sekhon, *Eur. Polym. J.*, 41 (2005) 2718.

37. I. Nicotera, L. Coppola, C. Oliviero, M. Castriota, E. Cazzanelli, *Solid State Ionics*, 177 (2006) 581.
38. T. Nagamoto, C. Ichikawa, O. Omoto, *J. Electrochem. Soc.*, 134 (1987) 305.
39. T.Y. Wu, H.C. Wang, S.G. Su, S.T. Gung, M.W. Lin, C.B. Lin, *J. Taiwan Inst. Chem. Eng.*, 41 (2010) 315.
40. T.Y. Wu, S.G. Su, S.T. Gung, M.W. Lin, Y.C. Lin, C.A. Lai, I.W. Sun, *Electrochim. Acta*, 55 (2010) 4475.
41. T.Y. Wu, B.K. Chen, L. Hao, K.F. Lin, I.W. Sun, *J. Taiwan Inst. Chem. Eng.*, 42 (2011) 914.
42. T.Y. Wu, B.K. Chen, L. Hao, C.W. Kuo, I.W. Sun, *J. Taiwan Inst. Chem. Eng.*, 43 (2012) 313.
43. T.Y. Wu, S.G. Su, S.T. Gung, M.W. Lin, Y.C. Lin, W.C. Ou-Yang, I.W. Sun, C.A. Lai, *J. Iran. Chem. Soc.*, 8 (2011) 149.
44. T.Y. Wu, I.W. Sun, S.T. Gung, B.K. Chen, H.P. Wang, S.G. Su, *J. Taiwan Inst. Chem. Eng.*, 42 (2011) 874.
45. T.Y. Wu, S.G. Su, H.P. Wang, I.W. Sun, *Electrochem. Commun.*, 13 (2011) 237.
46. T.Y. Wu, L. Hao, C.W. Kuo, Y.C. Lin, S.G. Su, P.L. Kuo, I.W. Sun, *Int. J. Electrochem. Sci.*, 7 (2012) 2047.
47. T.Y. Wu, S.G. Su, Y.C. Lin, H.P. Wang, M.W. Lin, S.T. Gung, I.W. Sun, *Electrochim. Acta*, 56 (2010) 853.
48. T.Y. Wu, B.K. Chen, L. Hao, Y.C. Peng, I.W. Sun, *Int. J. Mol. Sci.*, 12 (2011) 2598.
49. T.Y. Wu, I.W. Sun, S.T. Gung, M.W. Lin, B.K. Chen, H.P. Wang, S.G. Su, *J. Taiwan Inst. Chem. Eng.*, 42 (2011) 513.
50. T.Y. Wu, I.W. Sun, M.W. Lin, B.K. Chen, C.W. Kuo, H.P. Wang, Y.Y. Chen, S.G. Su, *J. Taiwan Inst. Chem. Eng.*, 43 (2012) 58.
51. M. Salomon, M. Xu, E.M. Eyring, S. Petrucci, *J. Phys. Chem.*, 98 (1994) 8234.
52. I.W. Sun, Y.C. Lin, B.K. Chen, C.W. Kuo, C.C. Chen, S.G. Su, P.R. Chen, T.Y. Wu, *Int. J. Electrochem. Sci.*, 7 (2012) 7206.
53. T.Y. Wu, S.G. Su, H.P. Wang, Y.C. Lin, S.T. Gung, M.W. Lin, I.W. Sun, *Electrochim. Acta*, 56 (2011) 3209.
54. I.W. Sun, H.P. Wang, H. Teng, S.G. Su, Y.C. Lin, C.W. Kuo, P.R. Chen, T.Y. Wu, *Int. J. Electrochem. Sci.*, 7 (2012) 9748.
55. T.Y. Wu, S.G. Su, K.F. Lin, Y.C. Lin, H.P. Wang, M.W. Lin, S.T. Gung, I.W. Sun, *Electrochim. Acta*, 56 (2011) 7278.
56. C.W. Kuo, C.W. Huang, B.K. Chen, W.B. Li, P.R. Chen, T.H. Ho, C.G. Tseng, T.Y. Wu, *Int. J. Electrochem. Sci.*, 8 (2013) 3834.
57. T.Y. Wu, L. Hao, P.R. Chen, J.W. Liao, *Int. J. Electrochem. Sci.*, 8 (2013) 2606.
58. M. Ulaganathan, S. Sundar Pethaiah, S. Rajendran, *Mater. Chem. Phys.*, 129 (2011) 471.
59. S. Ramesh, G.P. Ang, *Ionics*, 16 (2010) 465.
60. S. Ahmad, H.B. Bohidar, S. Ahmad, S.A. Agnihotry, *Polymer*, 47 (2006) 3583.